GEOLOGY AND PETROGENESIS OF THE ROCKS AROUND SHINTAKU AREA, SOUTHEAST LOKOJA, NORTH CENTRAL, NIGERIA

by

ADEJARE BARAKAT ENIOLA

GLY/14/2246

Department of Geology

Faculty of Science

Federal University Oye-Ekiti, Ekiti State, Nigeria.

February, 2019.

GEOLOGY AND PETROGENESIS OF THE ROCKS AROUND SHINTAKU AREA, SOUTHEAST LOKOJA, NORTH CENTRAL, NIGERIA

by

ADEJARE BARAKAT ENIOLA
GLY/14/2246

A PROJECT WORK SUBMITTED TO THE DEPARTMENT OF GEOLOGY, FACULTY OF SCIENCE, FEDERAL UNIVERSITY OYE-EKITI

IN

Partial Fulfilment of the Requirements for the Award of Bachelor of Science (B.Sc.) Degree in Geology

February, 2019.

Certification

This is to certify that the research project on the GEOLOGY AND PETROGENESIS OF THE ROCKS AROUND SHINTAKU AREA, SOUTHEAST LOKOJA, NORTH CENTRAL, NIGERIA was actually carried out by ADEJARE BARAKAT ENIOLA with matriculation number GLY/14/2246 under the supervision of E. C. CHUKWU.

The work has been approved as meeting the required standard for the award of Bachelor of Science (B.Sc.) Degree of the Department of Geology, Faculty of Science, Federal University Oye-Ekiti, Ekiti State, Nigeria.

Signature..... Date.....

Project Supervisor

Signature..... Date.....

Head of Department

Prof S. A. Opeloye

Signature..... Date 25/02/19.

External Examiner

Dedication

I dedicate this work to Almighty Allah who has been the source of my strength throughout this program and the course of this project. I also dedicate this work to my Parents, Mr. and Mrs. Adejare, who encouraged me all the way and gave all it takes to finish that which I have started. To all my siblings and friends, I dedicate this work to you, too.

Acknowledgements

Overall appreciation goes to Almighty God who has provided all that was needed to complete this Project.

My deepest gratitude goes to my supervisor, E. C. CHUKWU, whose contribution and constructive criticism has pushed me to expend the kind of efforts I have put in to make this work as original as it can be. I thank him for making me experience true research and expanding my knowledge on the subject matter.

My utmost regards go to my parents who gave me their financial support to ensure the completion of this work. I also appreciate my siblings and my supportive best friends who stayed with me to make this work a successful one.

TABLE OF CONTENTS

List of Figures

List of Tables

Appendixes

Abstract

The study area is part of the Basement Complex of Central Nigeria. The study aims at identifying the rock types and using major oxides for interpretating petrogenesis of the rocks. Geochemical analysis of eight samples were done using X-Ray Flouresence Technique (XRF). ACF diagram, al-alk versus Niggli c diagram, Na_2O/Al_2O_3 versus K_2O/Al_2O_3 diagram, were all employed in determining/interpreting the rock types, protolith and mineral assemblages to ascertain the metamorphic facies attained by metamorphic rocks. The major rock units in the area comprise of Granite, Migmatite Gneiss, Granite Gneiss and Schist. Evidence shows that the rocks are deformed and were intruded by the granitic plutons. Modal analysis reveals the existence of feldspar as deformed porphyroblast in a groundmass of quartz and biotite within the Granite Gneiss. The Granite is composed of quartz (25-35%), plagioclase (15-20%), orthoclase (10-20%), microcline (5-25%), biotite (15-20%) and accessory minerals. The gneiss displayed a granoblasitic texture while the schist and gneisses exhibit planar and linear structures. Variation in structural trend and mineralogical composition is due to the series of deformational activities which has affected the rocks during geologic time. The foliation trend which trends majorly NE/SW supports earlier arguments that the event that produced these rocks are Pan Africa in age (600±50Mya).

CHAPTER ONE

1.0 Introduction

The area is bordered in the north by the River Benue, in the west by the River Niger and falls under the southeast quadrant of Topographical Map-Sheet 247 of the Nigerian Ministry of Lands and Surveys. The area covers Kogi State, and Benue State, Nigeria.

The area has an average range of elevation of 80m to 170m (250ft to 550ft). But there are also topographic lows and highs, which are respectively characterized by quaternary alluvium that adjoins the River Benue in the south, and a ridge of sediments which flanks the Basement Complex in the East. The ridge of sediments on the eastern portion is about 304m (1000ft) above mean sea level, while the Basement Complex area has an intermediate topography.

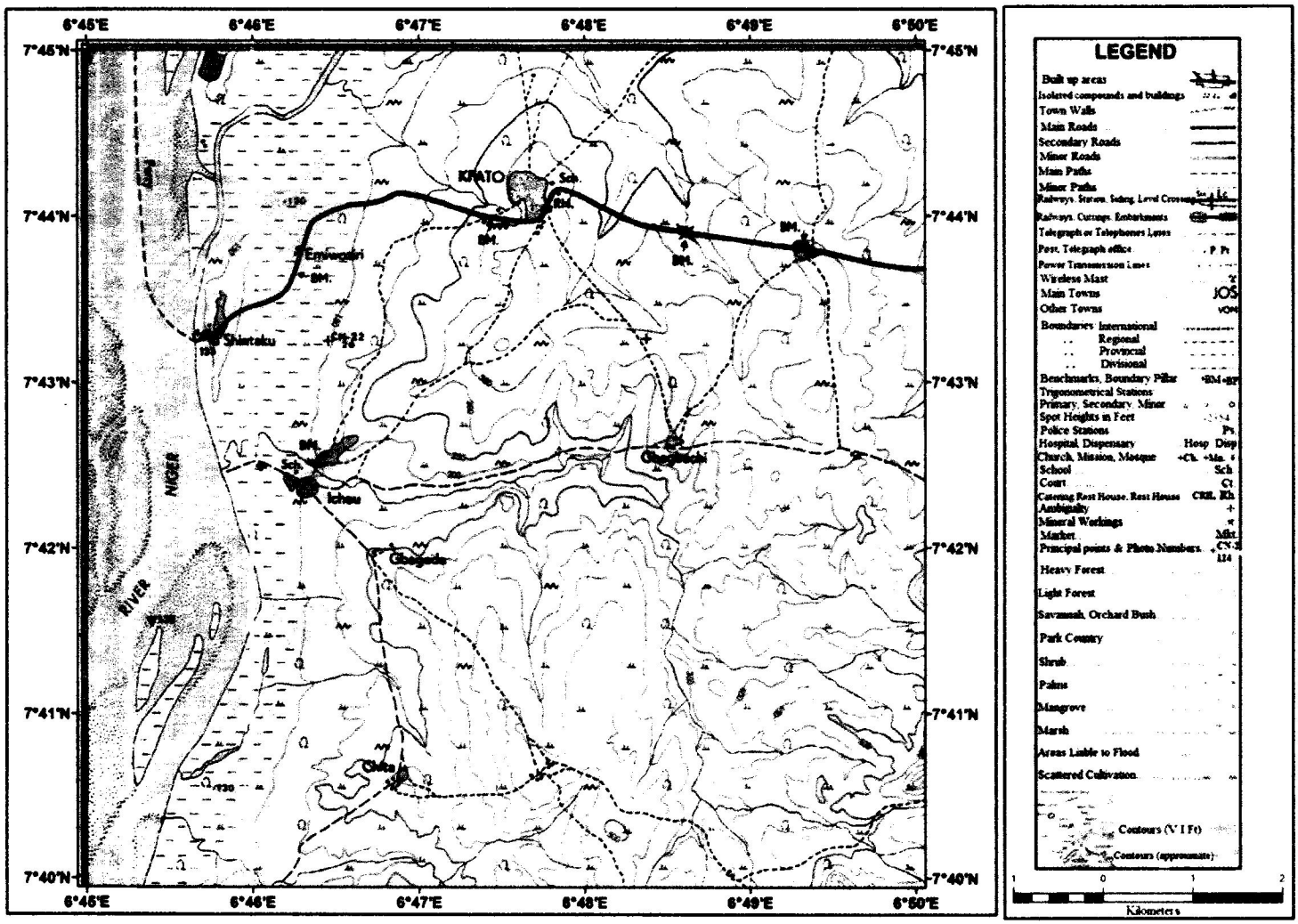

Figure 1: Topographical map of the Study Area

1.1 Aim and Objectives of the study

The major aim is to determine the geology and petrogenesis of the rocks in Shintaku area of south-east Lokoja. The following are the objectives:

i. Detailed geological field mapping of the Shintaku area
ii. Geochemical analysis of the samples obtained from the Shintaku area.
iii. Using the result of the geochemical analysis (major oxides) to interprete the petrogenesis, and mineral assemblages of the rocks in the area.

1.2 Scope of the study

The work entails carrying out a detailed geological field mapping of Shintaku area, south-east Lokoja, analysing the rock samples and interpreting the geochemical events in the study area.

1.3 Relevance of the work

Using the major oxides from the geochemical analysis (XRF) to describe the petrogenesis of the rocks which facilitates the understanding of the metamorphic transformations. The interpretation of ACF, Na_2O/Al_2O_3 vs K_2O/Al_2O_3, al- Alk vs Niggli c, and Na_2O+K_2O vs Silica plots will further investigate the petrogenesis of the transformed rocks. The Geology of the area will also be established. All these will help in the production of a true metamorphic/geologic map of the area.

1.4 Location, Extent and Accessibility of the Area of Study

Lokoja, the confluence of River Niger and Benue is located between latitudes $7°45^1$ and $7°53^1$N and longitudes $6°39^1$ and 6°48N. The study area Shintaku of South –East Lokoja lies between latitudes $7°40^1$N and $7°45^1$N, and longitudes $6^0$45'E and $6^0$50'E. It is underlain by the Basement Complex, which comprises mainly Quatzo-feldspathic granite, Gneisses and Schists.

A network of all season roads that connects the main parts of Lokoja to Shintaku makes the area accessible at all times and the rivers can be crossed by boats and ferries to the area, too.

1.5 Climate

Lokoja is characterized by two distinct seasons namely, the rainy and dry seasons. The rainy season commences in April and lasts till October, while the dry season is from November to March. Based on meteorological reports (Federal Ministry of Aviation, 2007), the annual average rainfall ranges between 1000 mm and 1500 mm, and the mean annual humidity is about 70%. The annual average temperature is 27°C, with annual average sunshine of 6.7 hours per day.

1.6 Vegetation

Vegetation of the area is of the guinea savannah type. The trees in the area has larger stems and and fewer leaves. They store water in the stem and prevent its transpiration through the leaves. This is as a result of the climatic condition of the area (ng.geoview.info).

1.7 Soils in the study area

The soil in the study area is fluviatile sands which formed from the weathering of the basement rock around the study area and the sands are also of dried river. The soils in the area support food crops and agricultural activities whereas the sands are used for construction purposes.

1.8 Occupation of the inhabitants of the Study Area.

As a result of the presence of the River (River Niger) cutting across the settlements in the study area, the inhabitants are engaged in fishing. The water from the river is also being used in watering the vegetable crops planted in the study area. This has encouraged grazing of livestock and cultivation of different types of crops in the area. The abundant water bodies and sufficient rainfall during the wet season encourage farming activities and rearing of livestock and other commercial activities like buying and selling of agricultural products.

CHAPTER TWO

2.0 Literature Review

The geologic setting comprises an assemblage of heterogeneity of rock types within the study area with division of the sedimentary terrain, the Basement Complex rocks and the igneous intrusive (Adeleye, 1976). It has a sedimentary terrain which comprises outcrops of light colour sandstones. Some parts of the sediments have been weathered and intensely lateritized. In consequence, bands and pockets of laterites and ferruginized sandstones exist. The banks of some big streams are bordered with boulders of sandstone while most hand specimens were collected from fossil bearing boulders. Colour changes in the various samples of the medium-grained sandstone are from light to grey, brown, reddish brown and dark brown. These colour variations reflect different degrees of ferruginization and/or laterization (Adeleye, 1976).

These sediments, deeply weathered, occur east of Nyankpo area also cover the entire Emi-Eronu, in the Northeastern portion of the study area. The prominent escarpment in the topographic map showing a range of hills of height about 250m (825ft) constitutes the easterly boundary of the Basement Complex. The degree of weathering and ferruginization of the sediments indicates a considerable similarity to the characteristic of the Upper Coal Measures. This gives credence to the result of previous geological mapping of the area by Ekwueme (1981) in which the sedimentary terrain of this area has been broadly identified as the Coal Measures, of Campanian-Maastrichtian age. The Northern fringe of the study area is delimited by Quaternary Alluvium which adjoins the southern bank of the River Benue. This portion bears little or no good outcrops, but constitutes favourable soil for agriculture.

The Basement complex portion consists of a variety of Schists ranging from quartz-bearing mica-Schists to quartz-free schist (Rahaman, 1976). Samples of the quartz-mica schist are characterized by white and dark bands which respectively show the preferred alignment of quartz and mica (biotite-muscovite) minerals. Other types of schists in the area are staurolite schist and Cordierite-Tourmaline schist which have been affected by the intrusion of olivine gabbro and granite bodies respectively (Cratchley and Jones, 1965). A discrete exposure of gabbro outcrop has an approximate extent of 15m x 20m; and is contiguously located with the Straurolite Schist, with a minimum separation of about 40m. The actual extent and thickness of the olivine gabbro would be estimated from the quantitative interpretation of gravity and magnetic data. Adjoining the Cordierite-Tourmaline schist westwards, are the Granite gneiss and migmatite which have been

subjected to intense granitic and pegmatitic intrusions. The Bouguer anomaly and Free-air anomaly profiles simultaneously indicate density and topogragphic changes and offer themselves to delineation markers at borders of changing rock types (Ojo and Ajakaiye, 1976). Major lithologic boundary outlines synergize or fall into phase with axes of inflexion of the Bouguer anomaly, as well as the Free-air anomaly especially with consistent topography (Telford, et al, 1976).

2.1 Regional Geology/Tectonic setting

Nigerian Pan – African Basement

The Nigerian Pan – African Basement is, on the basis of rock types, divided into three units Fitches et al., (1985); Ajibade et al., (1987), thus: The gneisses and migmatites with entrained supracrustal relics whose metamorphism is generally in the amphibolites facies grade. These rocks are mainly quartzites, amphibolites, calcareous rocks, biotite-hornblende gneisses, quartz schist and Biotite-hornblende schist.

The Schist belts: Composed of low-medium grade, deformed, supracrustal assemblages whose metamorphism is in the green schist facies, the belts are considered to be Upper Proterozoic rocks which have been infolded into migmatite gneiss complex. The schist belts are best developed in the Western half of Nigeria and are made up of poilitic and semi poilitic schist and phyllites, quartzites, conglomerates, iron formations, marbles, calc-silicate rocks and subordinate meta igneous rocks (Adekoya, 1996). These diverse rock types occur in varying proportions in the different belts.

The granitoid plutons of the Older Granite suite are considered as syntectonic to late tectonic Pan-African granitoids. They intrude both the migmatite gneiss complex and the schist belts. Earlier granitoids are foliated calc – alkaline granodiorite intrusions, while later undeformed post tectonic intrusions are monzonitic, sub alkaline to alkaline in character (McCurry,1989). Other rock varieties are: diorites, gabbros, charnokites and late tectonic high level volcanic and hypabysal rocks. The basement is also on the basis of spread and proportion of the rock suites divided into two provinces Ajibade et al. (1987). The Western province, approximately west of latitude 80 E,

comprising the schist belt in a predominantly migmatite gneiss Older basement, and the whole is intruded by large volumes of Pan-African granites and Mesozoic Younger Granites.

The Nigerian basement is on the basis of geochronology shown to be polycylic and include rocks of Archean (>2500); Ma) Eburmean (2000 ± 200Ma). (Turner, 1983; Fitches et al., 1985: Ajibade, (1989).

However the age of the last orogenic cycle especially as it affects the schist belts was a subject of controversy. Turner, (1983) considered the older schist belt as Kibaran (1100±200 Ma), and explained that the Pan-African tectonics imposed the N-S structural trends, and its magmatism led to the emplacement of granites and charnokites; and its thermal activity set mineral ages in the 500 – 600 Ma range in rocks in the area. He also considered Pan – African sedimentation to be uncertain in character and extent. He however, stated, "Deposits of Pan – African age are probably represented in the Northern Nigerian schist belts only. Fitches et al., (1985) supported this view with their work on Maru belt, which they considered to be part of the Kibaran basin. However Ajibade et al. (1987) regards the Kibaran event as questionable and not a major tectonic event in Nigeria. The late Proterozoic to early Phanerozoic Pan – African Orogenic - cycle (750 – 450 Ma) is generally believed to be responsible for the emplacement of large volume of granitoids and the resetting of mineral ages in virtually all rocks types in the basement Ajibade et al. (1987).The basement is intruded by Mesozoic alkaline ring complexes of the Jos Plateau, (Younger Granites), and uncomformably overlained by Cretaceous to Recent sediments.

The Nigerian schist belts occur in a 300 to 400 km wide zone, and predominantly west of longitude 80 E, which trends NNE, parallel to the boundary between the Pan – African province and the West African Craton, Turner (1983); Fitches et al. (1985): Ajibade et al. (1987); Adekoya (1996). The Schist belts zone is flanked by migmatites – gneisses – granites terrain, to the East and West, and the same terrain separate the individual belts within the zone Turner, (1983); Ajibade et al., (1987). The schist belts are believed to be metasedimentary – volcanic, deformed, low grade (green schist facies) rocks that fall into two age groups. The earlier group for example, Maru and Kushaka belts contain assemblages of mafic igneous rocks, phylitic schist and phyllites, banded iron formation and locally coarse – grained clastics and carbonate rocks. These belts are intruded by

granitic plutons belonging to the Pan – African magmatic suite. They are dated at approximately 1,100 Ma and are thought to belong to the Kibaran ensialic processes, (Fitches et al.1985). The later group of schist belts. For example, Anka Wonaka, Karu and Kazaure belts, are characterized by coarse to fine grained clastics, insignificantly mafic igneous rocks, and absence of central granite plutons. These schist belts are believed to belong to the Pan – African marginal basin development (Turner,1983; Fitches et al.1985). However, the Nigerian Pan – African schist belts are believed to have evolved by plate tectonic processes. They are described as been deposited on a back – are basin, which developed after the onset of subduction at the cratonic margin at about 1000 Ma. Closure of the ocean at the cratonic margin about 600Ma and crustal thickening to the East led to the deformation and metamorphism of the sediments (Ajibade et al.,1989).

The Older Granites

The Older Granites of Nigeria occur in all parts of the Nigerian basement and the extent of this Pan – African plutonism is still largely unknown (Ajibade et al., 1987). The Older Granites are intrusions emplaced by stopping and diapiric processes Fitches et al., 1985). They are generally regarded as late to post tectonic with respect to the main deformation of the Pan – African tectonism. The Older Granites suite include a wide spectrum of rocks, which includes: monzonite, adamellite, tonalite, granodiorite, granite, syenite and charnokitic rocks. These plutons are products of magma genesis at levels substantially below the present exposure level. To them, Ajibade et al. (1987) ascribed a mantle origin with minor crustal contribution. The most gneissic of the rocks is reported to contain angular xenolithic schist from adjacent belt.

Pegmatites

Pegmatites are widely distributed throughout the Pre – Cambrian Complex in Nigeria (Jacobson and Webb., 1946)

Classsification of Pegmatites

(a) Based on mineralogy: It is possible to make a convenient sub-division of pegmatites accordingly, local variations in the environment and composition of the solutions inevitably results in anomalous variations. However, when considered as a whole the pegmatites fall into three main groups:-

i. Microcline – quartz pegmatites

ii Microcline – quartz – mica pegmatites

iii Quartz – mica veins.

(b) Based on regional distribution: The pegmatites are genetically connected with the Older Granites, and they may be divided into three groups according to their regional distribution in relation to the granites:-

i. Interior pegmatites (core pegmatites)

ii Marginal pegmatites (Hood pegmatites)

iii Exterior pegmatites (Root pegmatites)

Phases of mineralization

The solutions which gave rise to the pegmatites were exceedingly complex, and there are many factors which governed the precipitation of the solid phases, each varying in importance from place to place. It is to be expected therefore, that each pegmatite occurrence will posses it's own individual characteristics. This is undoubtedly so, but it is nevertheless possible to outline the general trends of differentiation of the pegmatitic liquor. It is difficult to choose a satisfactory nomenclature for the phases of mineralization in the Nigerian pegmatites, as the precise nature of the pegmatite solution is imperfectly known (McCurry, 1976).

The first phase of primary crystallization may be called magmatic and the final stage hydrothermal, but the exact nature of the solutions during the important transition period is uncertain (McCurry, 1976).

''Magmatic'' and rather less implied by ''hydrothermal''. The terms pneumatolytic and pneumatohydatogenic imply an important gas or vapour phase, the existence of which is problematical. It is for these reason that the second phase has been termed ''intermediate'' (McCurry, 1976).

The phases of mineralization in the Nigerian pegmatites are briefly outlined below:-

i. Magmatic to Epi-magmatic stage of pegmatite formation.

ii. Intermediate stage of pegmatite formation.

iii. The hydrothermal stage

Table 1: Generalized geochronology for the basement rocks of Nigeria (modified after McCurry, 1976).

AGE	GEOLOGIC TIME	EVENTS	ROCK TYPES
540+580 Ma	Late – Pan African	Uplift, cooling, faulting, high level magmatic activity	
650 – 580 Ma	Pan – African	Granitic instrusion, pegmatities and aplite development	Older Granites Magmatism
650 – 850 Ma	(Main phase)	Orogenesis: deformation, metamorphism, migmatisation and reactivation of pre-existing rocks	
800 – 1000 Ma	Katangan	Geosynclinal deposition, instrusion of hypersthenes – bearing rocks (charnockites)	Katangan Metasediments
1900 ± 250 Ma	Eburnean	Granite intrusion Orogenesis: folding metamorphism and reactivation of pre – existing rocks.	Eburnean granite
2500± Ma	Birimian	Geosynclinal deposition	Eburnean granite
2800 ± 200 Ma	Liberian cycle	Possible formation of banded Gneiss complex near Ibadan	
>2800	Dahomeyan	Crystalline Basement	

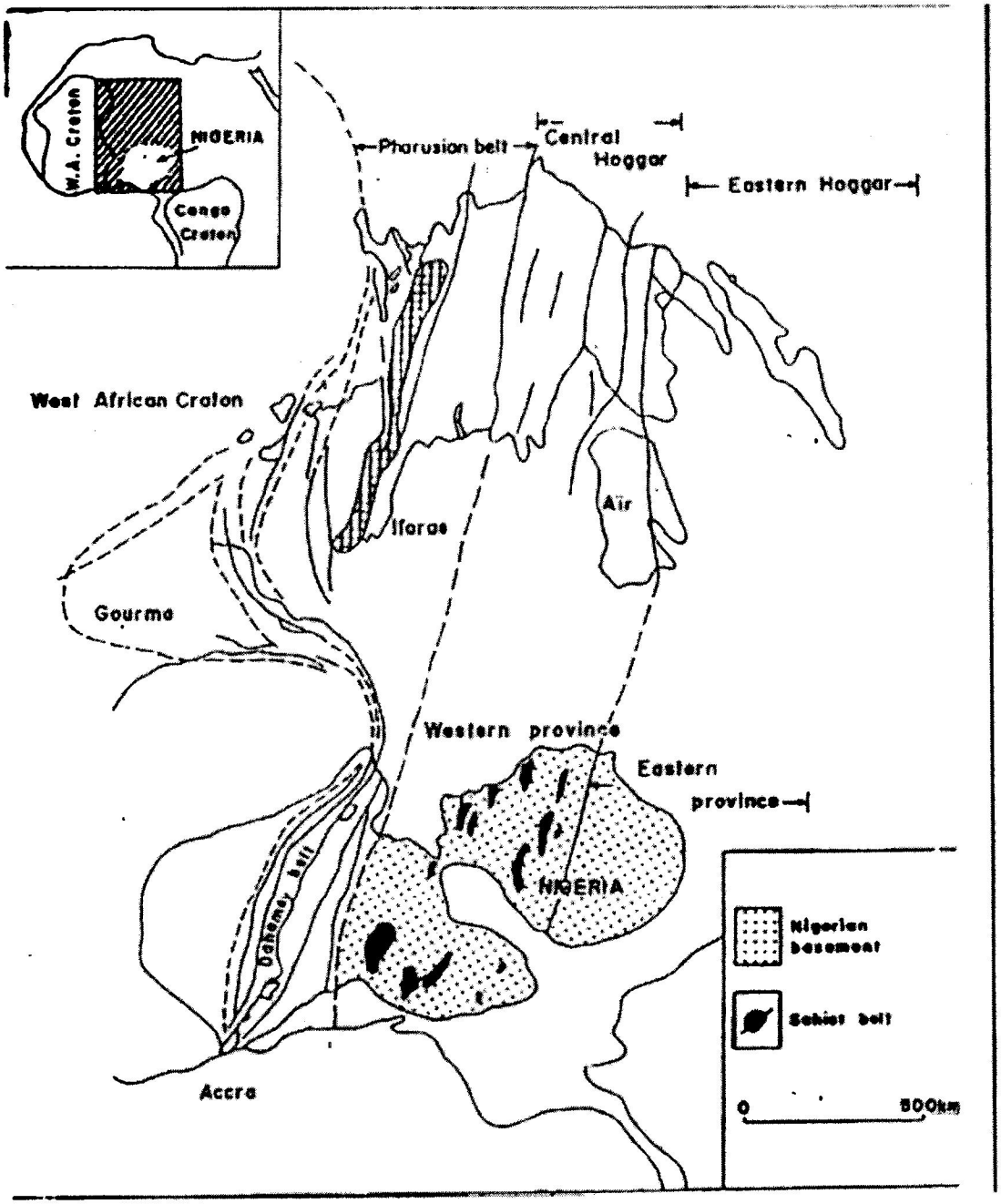

Figure 2: Geological map of the Pan-African belt east of the West African Craton showing the relative positions of the Nigerian basement and the Tuareg shield. (after Ajibade et.al., 1987).

CHAPTER THREE

3.0 Materials and Methods

The method of study adopted for the different aspects of this work include field operation. The field operations involve sample collection and the sampling methods. In this method, the rock samples were picked at a sampling density of two samples per location. Each rock sample was collected from each location in the study area and was lithologically described based on their field relationships after which it was labelled properly and put in a sample bag.

3.1 Methods of Data Collection

Geological mapping which is a very important process of making observations about rocks in the field and recording their locations on the topographical map so that a geological map can be produced was done.

The basic procedures followed for the geological mapping include the following:

i. Location of outcrop: noting the place the rock is found.
ii. Examination of outcrop: noting the type and features on the rock
iii. Plotting the field data on the map: this includes outcrops and structures.

Strike and dip measurement.

The strike and dip measurement is taken using the compass clinometers

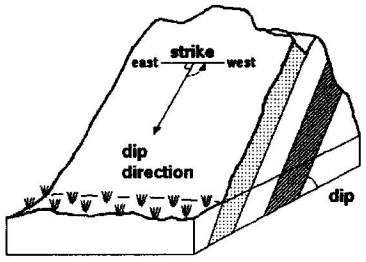

Figure 3: A sketch of the direction of strike, dip direction and dip (amount) on a typical dipping rock

3.2 Field work

The basic methods of geological mapping used is the reconnaissance mapping and detailed mapping. This can enlarge the scope of the local study by providing a specific picture of the region. This is the kind of mapping that was used in the Shintaku area mapping exercise. Reconnaissance

maps may therefore range from fairly complete geological maps to mere sketches that illustrate only the rock units and structure of the region. On getting to an outcrop the first thing that was done is put down the longitude and latitude at which the rock was encountered using the global positioning system(GPS) and the point was located on the topographical map, after which thegeological features on the rock are observed and recorded. If there is presence of planar surfaces on the outcrop strike and dip values were taken using the compass clinometer. Using the hand lens, the modal analysis of the minerals in the rock is done and recorded. Structural features were also recorded that is foliation trend, trend of veins and intrusions using the compass clinometer. Fresh samples were collected from the outcrop using the geological hammer and labelled properly using a marker. Finally, the photograph of the outcrop was taken, and we moved to the next location.

3.3 List of Major Materials/Equipment and Their Uses

Global Positioning System (GPS): The GPS was used to get the actual Longitude, Latitude and elevation at each location, the type used is Garmin, model GH7.

Geological Hammer and Chisel: Hammer as a hand-held instrument, was used to break down rocks mechanically to get fresh samples of rocks. While chisel allow the parting of rocks along its plane of weakness.

Compass Clinometer: The Clinometer is used to determine the strike and Dip (Fig.3). It is also used for determining the trend of the foliation on outcrops and for monitoring our bearing on the topographic map in order to know our location.

[illegible]: This is used for cutting the vegetation cover on the outcrop, especially where the [illegible] is not very accessible.

[illegible]: Used for taking photograph of structures, and other features on the outcrop.

Chisel

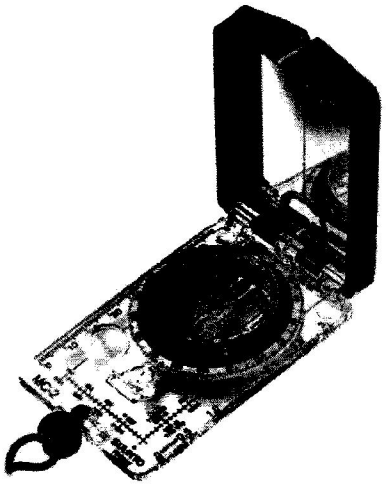

Compass clinometer

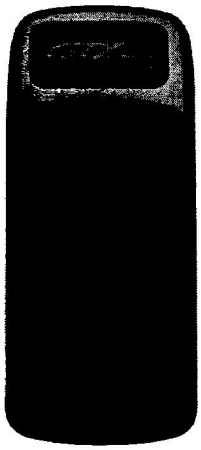

Global positioning System

3.4 Method and Processing of sample analysis

The method of the geochemical analysis used is the Energy dispersive X-Ray Fluorescence (EDXRF) instrumentation which is one of the general types of X-ray Fluorescence instrumentation used for elemental analysis applications. The name of the equipment is SKYRAY INSTRUMENT, Model: EDX3600B. EDX3600B X-ray fluorescence spectrometer applies XRF technology to conduct fast and accurate analysis of complex composition. The system detect elements between Magnesium (Mg, Z=12) and Uranium (U, Z =92) with high resolution and fast analysis.

The analysis of major and trace elements in geological materials by XRF is made possible by the behavior of atoms when they interact with X-ray radiation. An XRF spectrometer works because if a sample is illuminated by an intense X-ray beam, known as the incident beam, some of the energy is scattered, but some is also absorbed within the sample in a manner that depends on its chemistry. The incident X-ray beam is typically produced from a Rh target, although W, Mo, Cr and others can also be used, depending on the application. When this primary X-ray beam illuminates the sample, it is said to be excited. The excited sample in turn emits X-rays along a spectrum of wavelengths characteristic of the types of atoms present in the sample. The atoms in the sample absorb X-ray energy by ionizing, ejecting electrons from the lower (usually K and L) energy levels. The ejected electrons are replaced by electrons from an outer, higher energy orbital. When this happens, energy is released due to the decreased binding energy of the inner electron

compared with an outer one. This energy release is in the form of emission of characteristic X-rays indicating the type of atom present. If a sample has many elements present, as is typical for most minerals and rocks, the use of a Wavelength Dispersive Spectrometer much like that in an Electron Probe Micro-analyzer (EPMA) allows the separation of a complex emitted X-ray spectrum into characteristic wavelengths for each element present. Various types of detectors (gas flow proportional and scintillation) are used to measure the intensity of the emitted beam. The flow counter is commonly utilized for measuring long wavelength (>0.15 nm) X-rays that are typical of K spectra from elements lighter than Zn. The scintillation detector is commonly used to analyze shorter wavelengths in the X-ray spectrum (K spectra of element from Nb to I; L spectra of Th and U). X-rays of intermediate wavelength (K spectra produced from Zn to Zr and L spectra from Ba and the rare earth elements) are generally measured by using both detectors in tandem. The intensity of the energy measured by these detectors is proportional to the abundance of the element in the sample. The exact value of this proportionality for each element is derived by comparison to mineral or rock standards whose composition is known from prior analyses by other techniques.

Sample preparation

For non-homogeneous sample, sample is pulverised to fine homogeneous size and then pelletized. A second split of sample dried at 105°C sample is then fused in a platinum-gold crucible with a commercial lithium tetraborate flux. The molten material is cast in a platinum mold. Fused discs are analyzed by X-ray Fluorescence Spectrometer (XRF).This requires a minimum of 5g sample pulp.

Sample testing computer program is as follows:

1. Start
2. Initialization (calibration), using pure silver standard
3. Select the working curve according to the sample
4. Test sample
5. Output to Excel
6. End.

CHAPTER FOUR

4.0 Results and Discussions

4.1 Lithological Description

The major lithological units mapped in the study area include Granite, Porphyroblastic Gneiss, Migmatite Gneiss and Schist. Others include pegmatite veins and other minor intrusive such as quartz veins and quartzofeldspathic veins. Alluvium, laterite and soil occur as superficial deposit.

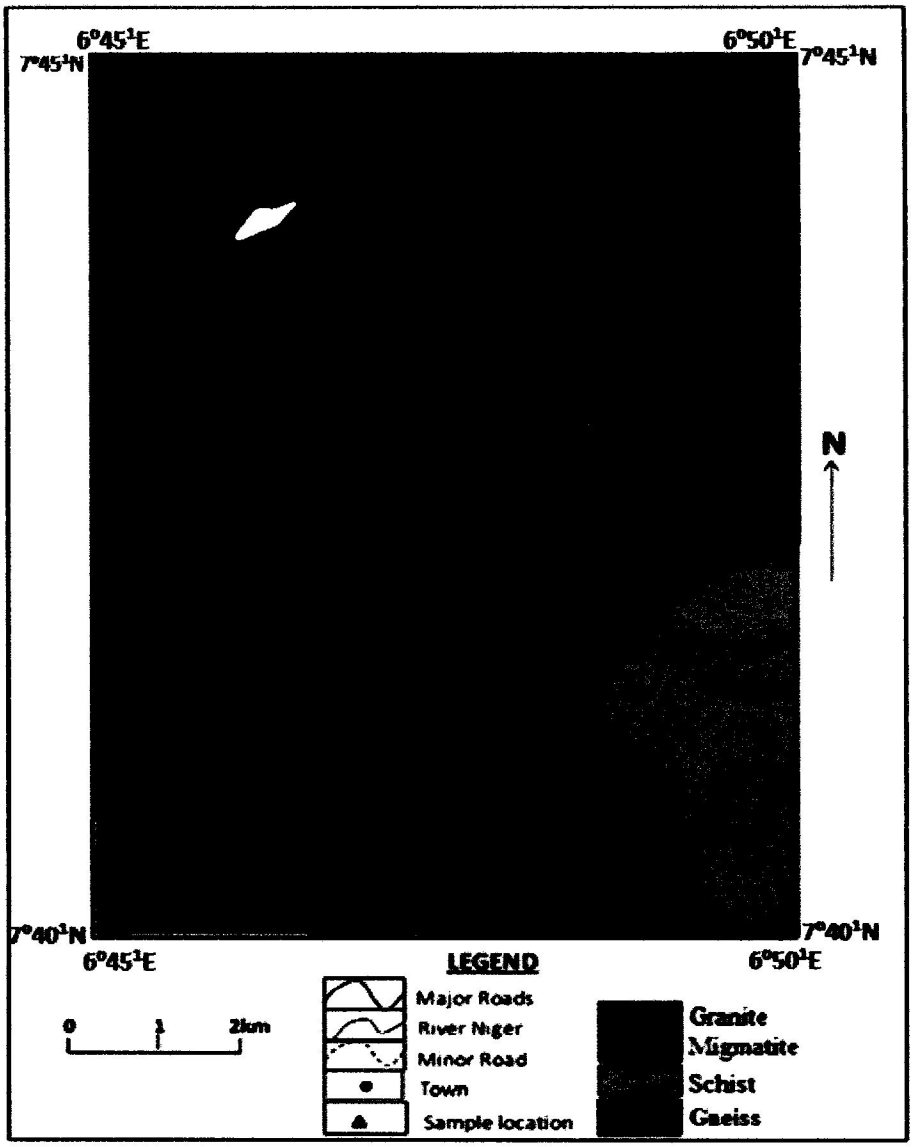

Figure 4.1: Geological map of the Shintaku area

Granite: ($6^0$46`43.0``E, $7^0$44`08.1``N)

The Granite in the mapped area occur around Emiwoziri, Kpata and Shintaku. They are **medium** to coarse grained texturally and are massive. They are characterized by quartz veins and **joints**. The rock displays a variety of coloured minerals in hand specimen which ranges from grey to brown and pink. Minerals such as quartz, feldspars, muscovite, biotite are present.

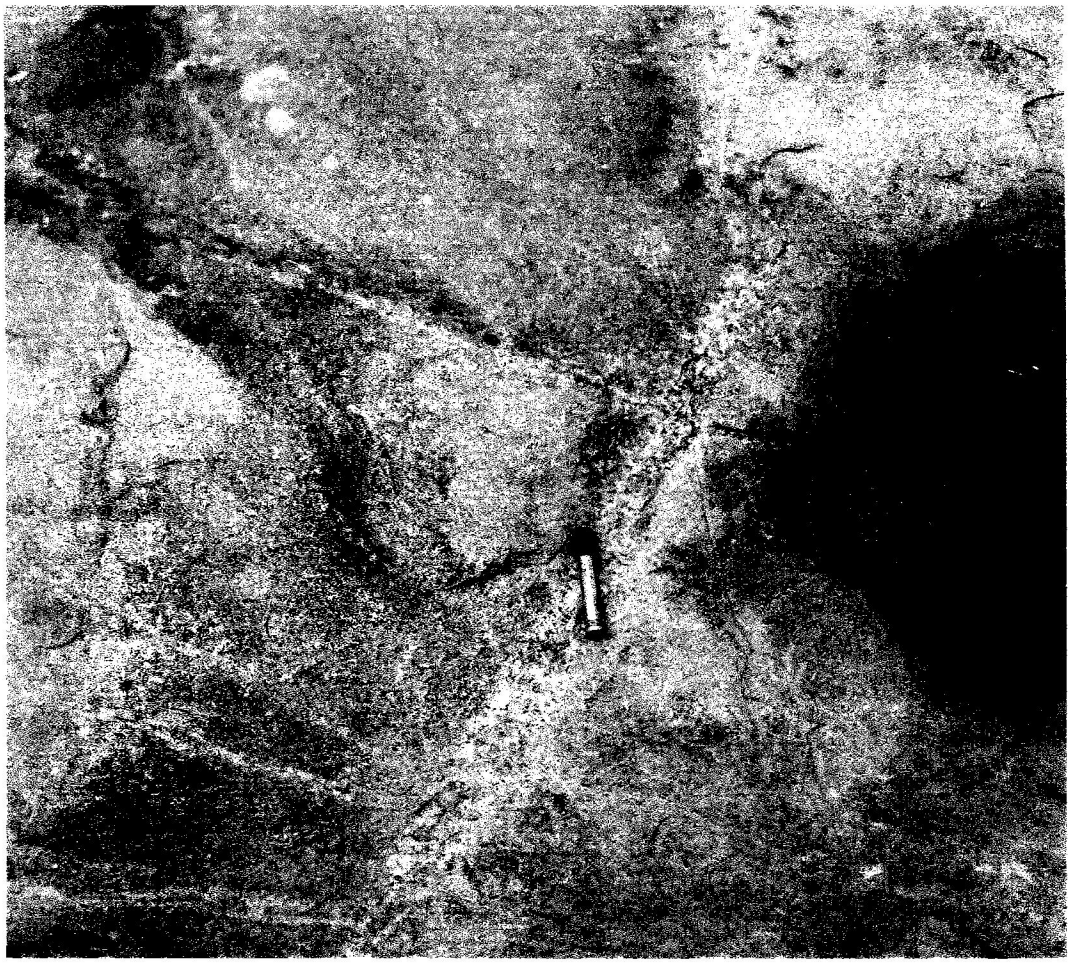

Figure 4.2: Photograph of Granitic outcrop at Emiwoziri

Granitic Gneiss: ($6^0$46`48.6``, $7^0$40`34.7``N)

This rock occurs at Chite. It is generally grey to dark in colour. Texturally, it is generally medium grained when fresh and coarse when weathered and observed under hand-lens. Mineralogically, the rock contains feldspars and quartz as the light coloured minerals and biotites as dark feromagnessian minerals. Feldspars occur as porphyroblast (1cm-3cm).

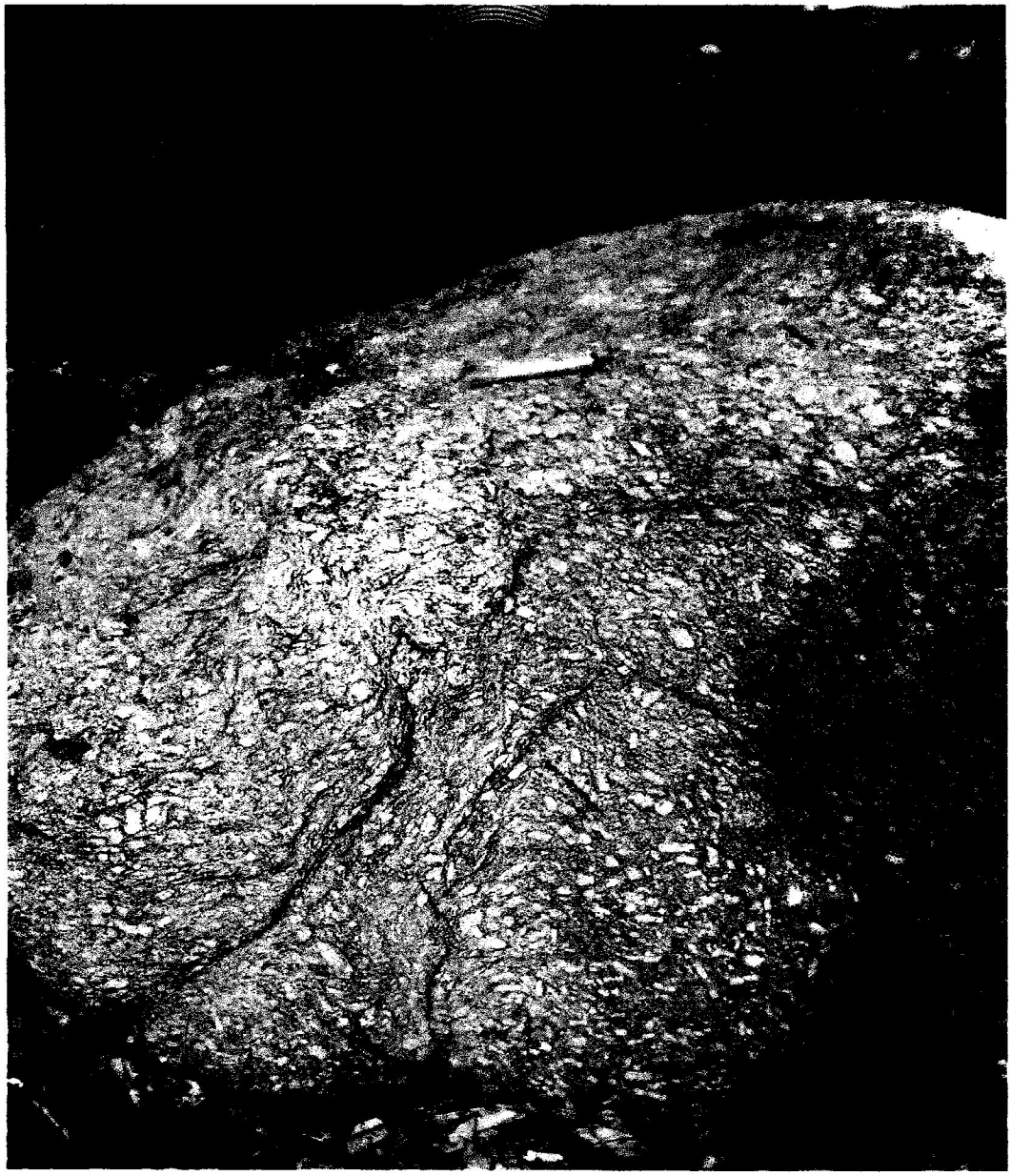

Figure 4.3: Photograph of Granite Gneiss at Chite

Migmatite Gneiss: ($6^0$46`51.8``E, $7^0$42`38.8``N)

The rock is found around Icheu and Shintaku. The colour variation on the rock ranges from grey to dark. It shows a mixture of igneous and metamorphic rock clearly showing its contact. They are intruded by veins and there is presence folds and foliations on the outcrops.Mineralogically, under hand lens, the rock contains biotite, quartz, feldspar and muscovite.

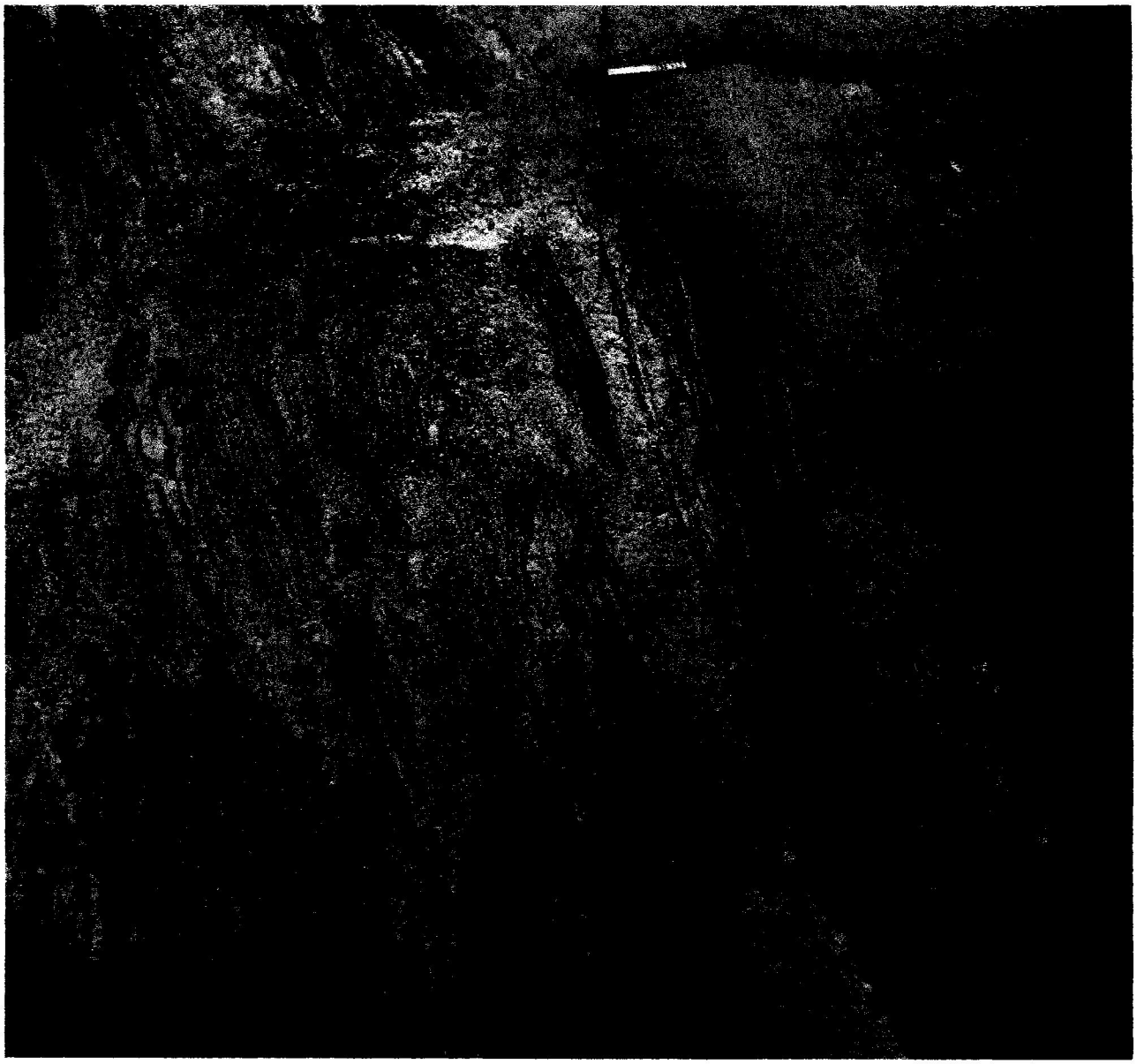

Figure 4.4: Photograph of migmatite gneiss at Icheu

Schist: ($7^0$42`30.6``N, $6^0$49`48.8``E)

The studied area is also made up of schists. The schists are foliated and folded, the foliation are characterised by the ferromagnesian minerals and quatzo-feldspathic minerals. Texturally, the rock is a medium to coarse grained rock showing a schistose cleavage/ texture.

Figure 4.5: Photograph of Schist at Emilafia

4.2 Structural Geology

The structural elements observed in the field include those formed due to brittle deformation (brittle structures) e.g. dykes and ductile deformation (ductile structures) e.g. folds.

a. **Faults**: Faults are fractures in bedrock along which there is a noticeable displacement. Most of the faults found in the study area are dextral faults.

Figure 4.6: Dextral fault on the exposure of Gneiss at Emiwoziri

b. **Folds:** These are structures where layerings are deformed without breaking so that the layering surfaces are curved but continuous. Folds are caused majorly by confining pressure. Examples of the fold found in the study area are open folds, isoclinal folds, and

recumbent folds. They occur in the Migmatite found in the western part of Shintaku,the study area.

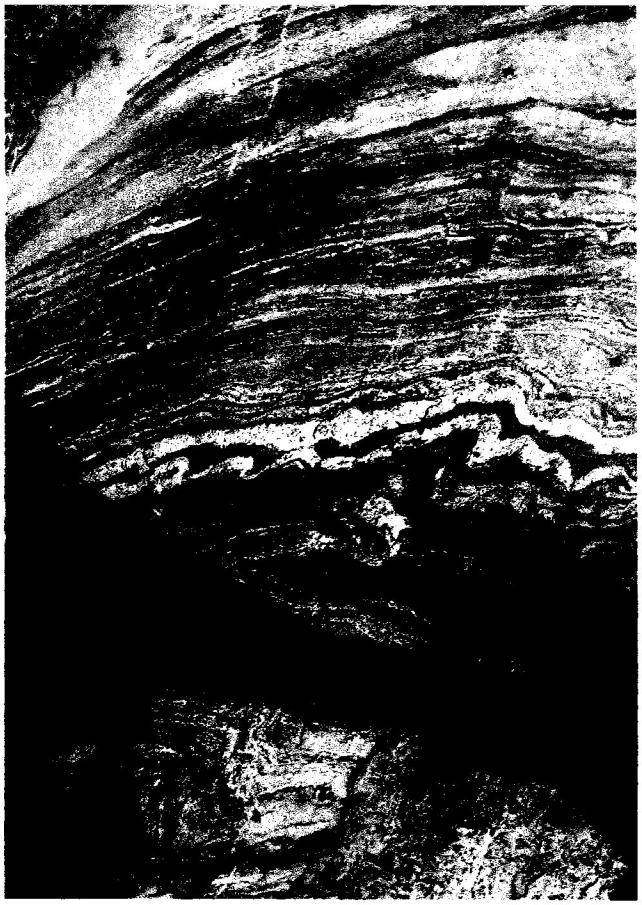

Figure 4.7: Ptygmatic fold on the exposure of Migmatite at Shintaku

Figure 4.8: Open fold on the exposure of Migmatite atKpata

Figure 4.9: Recumbent fold on the exposure of Migmatite atIcheu

c. **Intrusions**: This is caused by a body of magma flowing into a country rock through faults and joints and thereby crystallizes in this opening which may either run concordantly or discordantly to the host rock. Some of these intrusions contain magmatic or hydrothermal deposits. Examples of intrusions are dykes (discordant), veins and sills (concordant).

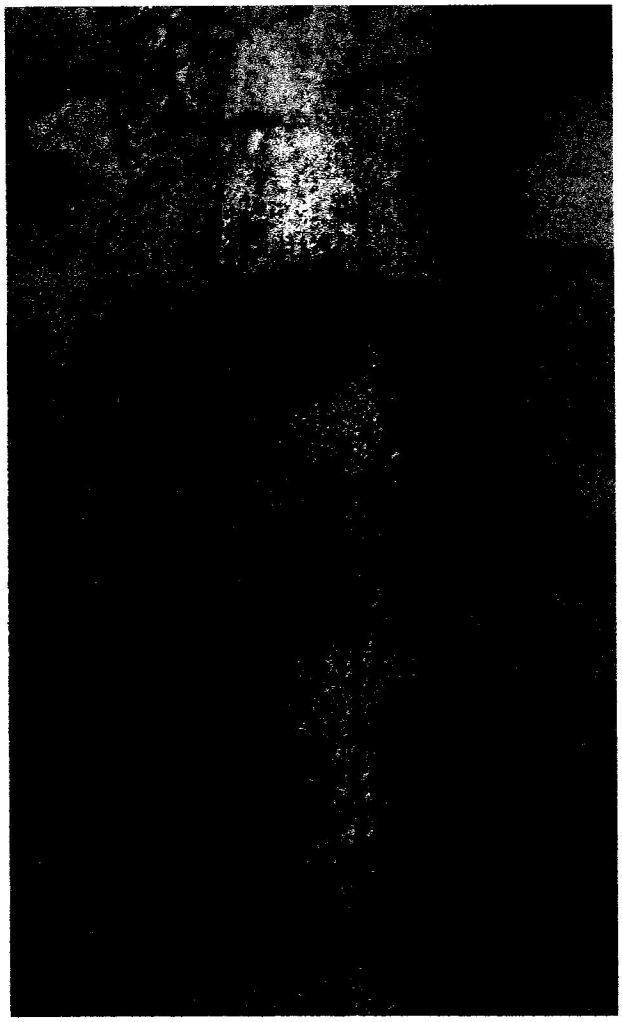

Figure 4.10: An intrusion of quatzo-feldspathic vein cutting through an exposure of Migmatite at Icheu.

Figure 4.11: A 4cm quatzo-feldspathic intrusion on the exposure of migmatite at Icheu.

Pegmatitic intrusion: This intrusion is formed by late stage cooling of magma which results in excessive large crystals of minerals. It is also granitic in composition and most of the pegmatitic intrusions host economic minerals such as tourmaline, tantalite, and beryl. These are

hydrothermal deposits. Most of the pegmatitic veins found in the study area run, NW-SE a few **run** NNE-SSW. They also occur majorly in banded gneiss and migmatite gneiss.

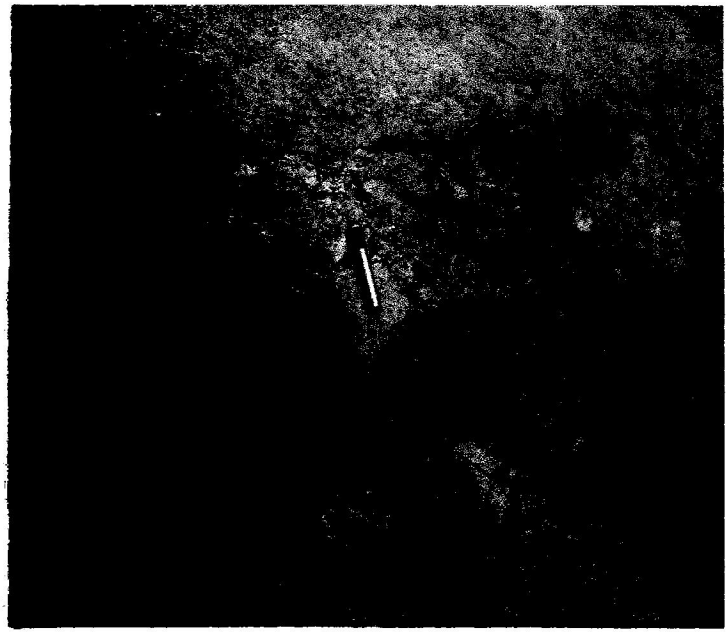

Figure 4.12: A pegmatitic vein trending NE-SW and marking the contact between the igneous and metamorphic feature on the exposure of Migmatite at Kpata

Figure 4.13: A Pegmatitic vein on the exposure of Migmatite at Icheu

Joints: These joints result from brittle fracture of the rock body as a result of tensile stress.These **tensile stresses either** were induced or imposed from outside, e.g. by the stretching of layers; the **rise of pore fluid** pressure as the result of either external compression or fluid injection; or the **result of internal stresses** induced by the shrinkage caused by the cooling or desiccation of a rock **body or layer whose** outside boundaries remained fixed.

Figure 4.14: Photograph of cross cutting joints on the Migmatite outcrop at Icheu.

4.3 Discussion

Using the Na_2O/Al_2O_3 versus K_2O/Al_2O_3 diagram, all the samples fall in the sedimentary and metasedimentary field (Fig. 4.15). This implies that the protoliths of the samples analyzed are sedimentary and metasedimentary rocks (Garrels and Mackenzie, 1971). The table below shows the calculated values for plotting the Na_2O/Al_2O_3 versus K_2O/Al_2O_3 diagram.

Table 2: Data used for plotting Na_2O/Al_2O_3 versus K_2O/Al_2O_3 diagram (see calculation as appendix 2)

SAMPLES	Na_2O/Al_2O_3	K_2O/Al_2O_3
EM 1	0.0009	0.3983
CHT 2	0.0026	0.2861
SK1Exp 2	0.0014	0.3468
KT6	0.0034	0.1722
EMLF 1	0.0007	0.2491
ICH3a	0.0003	0.0831
KT1	0.0012	0.3959
ICH6	0.0002	0.4425

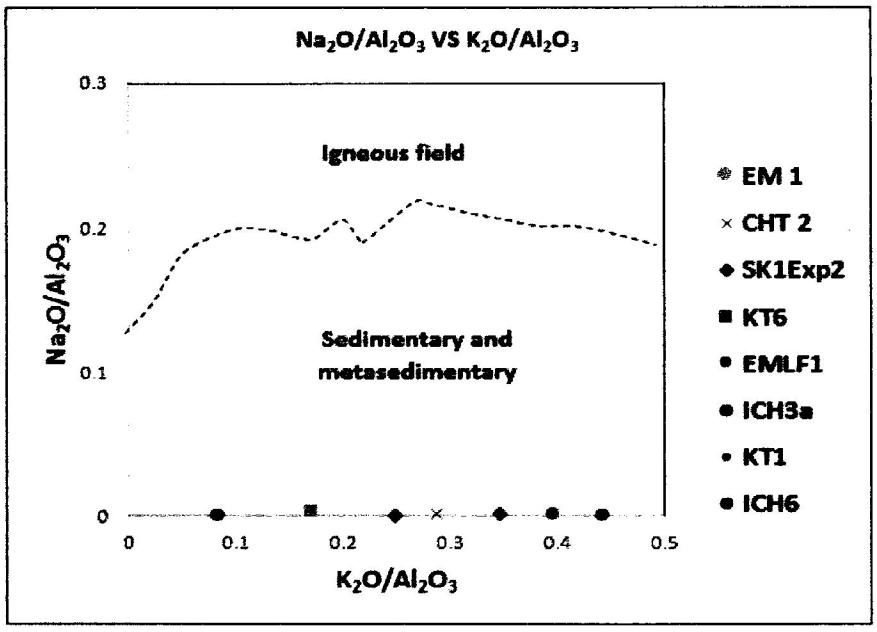

Figure 4.15: Na_2O/Al_2O_3 versus K_2O/Al_2O_3 diagram (after Garrels and Mackenzie,1971)

Table 3: The samples analysed and their lithology

SAMPLES	LITHOLOGY
EM1	Migmatite
CHT2	Granite Gneiss
SK1Exp2	Migmatite
KT6	Migmatite
EMLF1	Biotite Schist
ICH3a	Migmatite
KT1	Granite Gneiss
ICH6	Migmatite

EMLF1 (Biotite-Schist) falls in the Al-rich clays and shales field in the ACF diagram (Fig. 4.16). This schist is enriched in SiO_2 and Al_2O_3. The chemical composition of the schist indicates that they were derived from Al-rich clays and shales. As a result, they have high TiO_2/ Al_2O_3 and variable K_2O/Na_2O ratio. Low TiO_2 and Ni content of these metasediments suggest that felsic to intermediate debris were possibly mixed in the source rocks. The schist is a product of metamorphism of immature sediments which were deposited in an intracratonic extensional basin (Ekwueme, 2002).

A= $[Al_2O_3]$ - $[Na_2O]$ - $[K_2O]$

C= [CaO] - 10/3 $[P_2O_5]$ - $[CO_2]$

F= [FeO] + [MgO]

Table 4: Data used for plotting the ACF diagram (see calculation as appendix 2)

SAMPLES	A	C	F
EM 1	48.2	0.42	51.34
CHT 2	32.2	16.7	51.1
SK1Exp 2	23.8	39.9	36.1
KT6	37.5	32.8	29.7
EMLF 1	23.2	17.5	59.2
ICH3a	55.7	30.1	14.2
KT1	46.9	-0.5	53.7
ICH6	82.5	-2.6	20.1

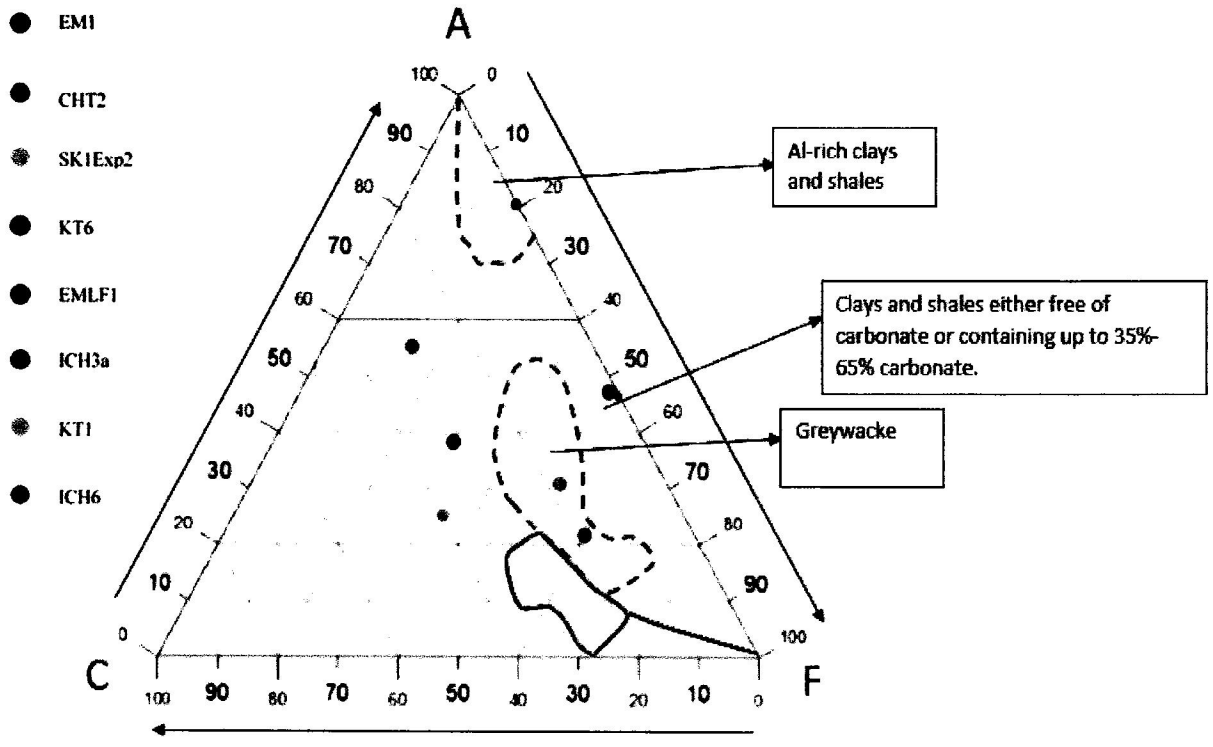

Figure 4.16: Plot of ACF diagram (Winkler 1967)

The alk versus Niggli c diagram (Fig. 4.17) indicates that the Schist, Gneiss and Migmatite are typical of igneous differentiation trend (Leake and Singh, 1986). Table 4 shows the calculated values for plotting the al-alk versus Niggli c.

Table 4: Data used in plotting al-alk versus Niggli c (see calculations as appendix 2)

SAMPLES		
EM 1	20.9	2.2
CHT 2	17.2	12.4
SK1Exp 2	4.3	45.5
KT6	24.8	23.9
EMLF 1	13.1	10.6
ICH3a	40.5	30.6
KT1	11	1
ICH6	30	2

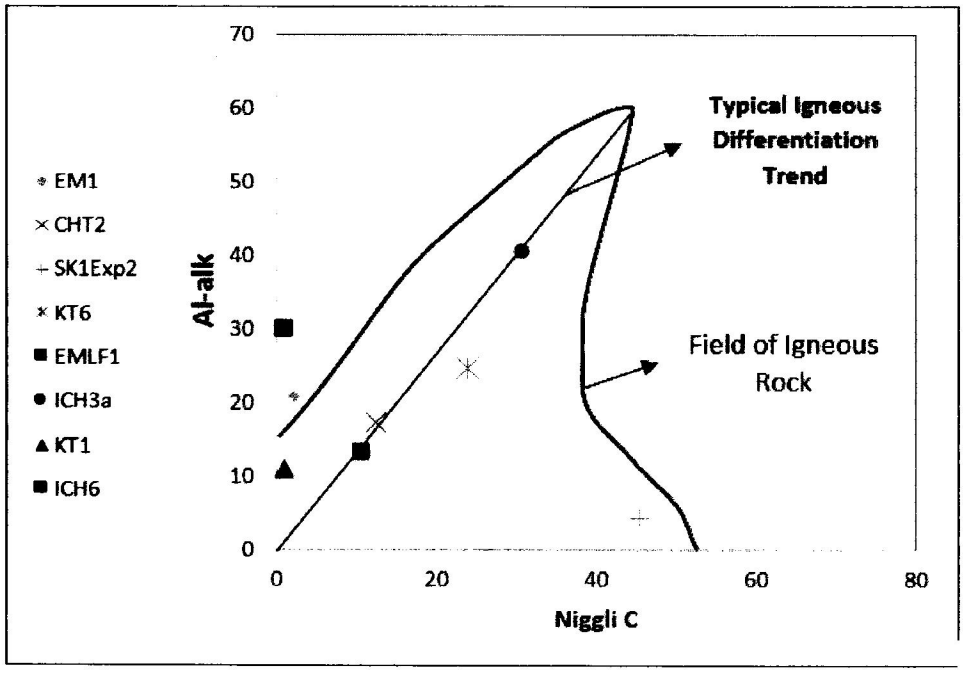

Figure 4.17: al-alk versus Niggli c diagram (after Leake and Singh, 1986)

The Na_2O+K_2O versus Silica diagram(Fig. 4.18) shows that all the samples analyzed were products of tholeiitic magma because the rocks has silica content (that is, silicic) and normative calculations shows the presence of quartz. The iron content in all the rocks ranges from 1.3-

24.2%. They arenot alkali magma because the result of geochemical analysis shows sodium in the range of (0.003-0.04%) (Appendix 1) which implies that the rocks are not sodium rich, which opposes the characteristics of alkali magma. The rocks are also iron and silica rich (Appendix 1) as opposed to alkali magma characteristics. They are not calc-alkali magma because the plot shows tholeiites and not intermediate between the tholeiites and alkali rocks which is contrary to the properties of calc-alkali magma. The Table 5 shows the data used in plotting K_2O+Na_2O versus SiO_2.

Table 6:Data used in plotting K_2O+Na_2O versus SiO_2(see calculation as appendix 2)

SAMPLE	Na_2O+K_2O	SiO_2
EM1	4.12	72.32
CHT2	3.36	57.43
SK1Exp2	2.5	25.5
KT6	2.1	66.1
EMLF1	3.5	35.2
ICH3a	1.02	72.8
KT1	3.34	76.8
ICH6	5.73	73.6

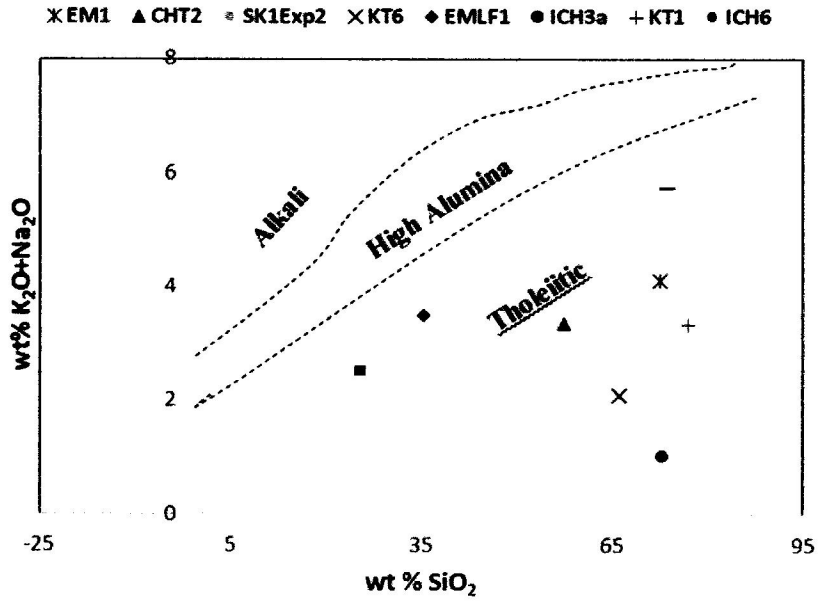

Figure 4.18: K_2O+Na_2O versus SiO_2(after Irvine and Baragar, 1971)

The major trends of the Foliation in the study area lies in NNE/SSW direction illustrated by the rose diagram (Fig. 4.19). This indicates that the rocks of the area were formed as a result of Pan African Orogeny (600±50Ma) (Ekwueme, 1983).

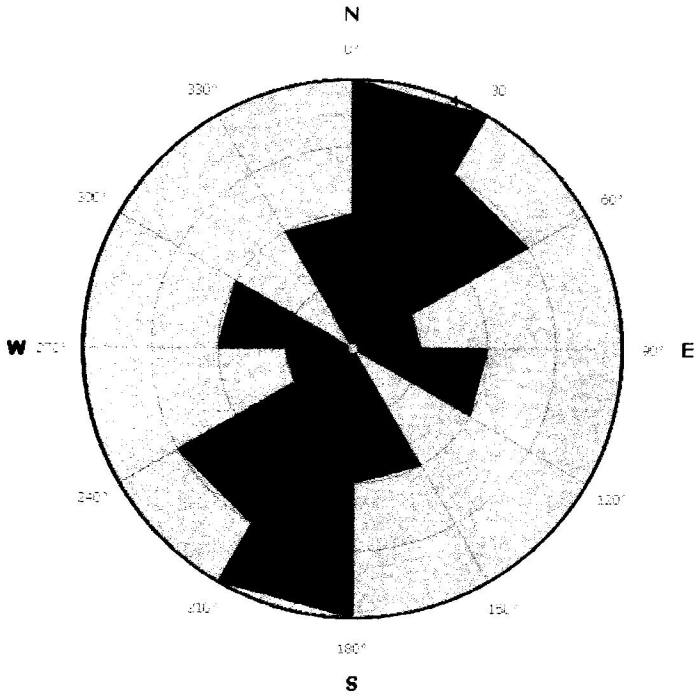

Figure 4.19: Rose diagram showing the major trend of foliation

Using the trend of joints illustrated by the rose diagram (Fig. 4.20), the major stress that affects the rocks of the Shintaku area is in E/W direction while the minimum stress is in NE/SW and NW/SE direction. Cross cutting Joints (Fig.4.14) indicates that the rocks of the studied area formed from different orogenic events. According to Mccurry (1971) and Danbatta (1999), the joints often result from contraction on cooling and are believed to be associated with a single episode of cooling and fracturing during epirogenic uplift.

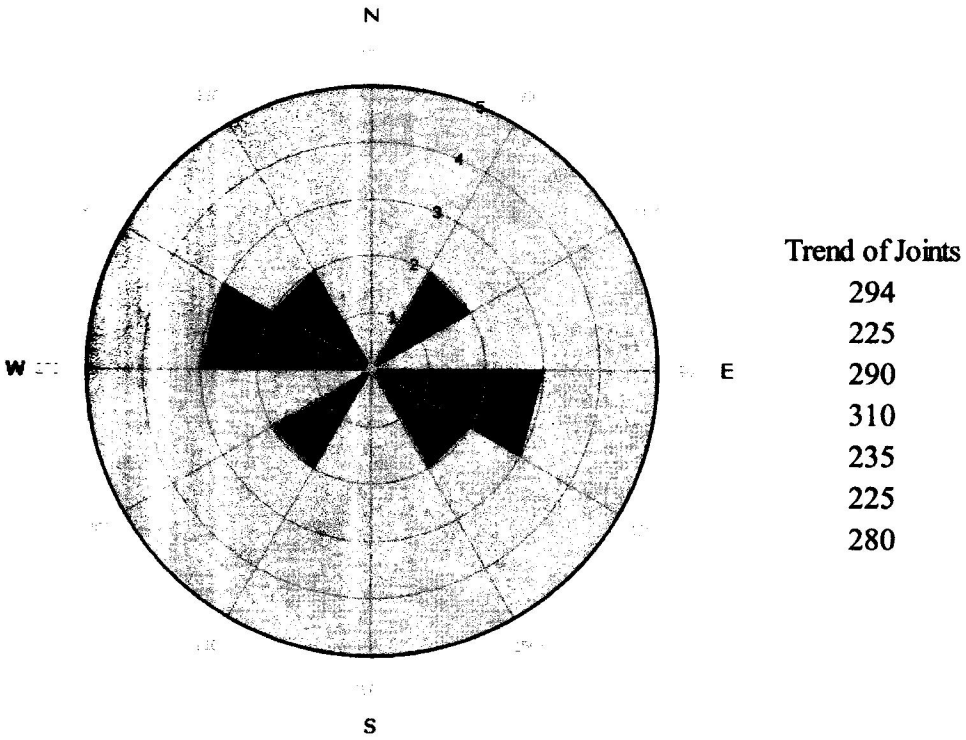

Figure 4.20: Rose diagram showing the major joint trend

The sequence of entry of the index minerals Garnet-Staurolite-Cordierite (EMI, KT1, CHT2 and ICH6) (Fig. 4.21) into the pelitic assemblages of the Shintaku area indicates that metamorphic facies ranges from Greenschist Facies to the Amphibolite facies which implies that the grade of metamorphism ranges from medium (formed at low pressure and low temperature) to high (formed at medium pressure and high temperature). The assemblages of the index minerals (that is, Garnet-Staurolite-Cordierite) shows that EMI, KT1, CHT2 and ICH6 belong to the Amphibolite Facies. The mineral assemblages (that is, Plagioclase-Muscovite-Andalusite-Sillimanite) (Fig.4.19) in SK1Exp2, KT6 and ICH3a indicate the Greenschist Facies which is a medium grade of metamorphism (formed at low pressure and low temperature).

However, since the assemblage Quartz+Muscovite+Staurolite is present in the rock (EMLF1), bathozone of Carmichael (1978) have been attained. The presence of index minerals; Almandine Garnet, Staurolite and Cordierite as shown in (Fig.4.21) indicates that the rocks analyzed have undergone prograde regional metamorphism(Winkler, 1965). The coexistence of Cordierite and Almandine which occurred in the Shintaku area is significant and indicate that metamorphism took place at intermediate pressures and that high temperature were attained which led to the

formation of Migmatite as a result of partial melting (anatexis) in some of the rocks (Winkler, 1965).

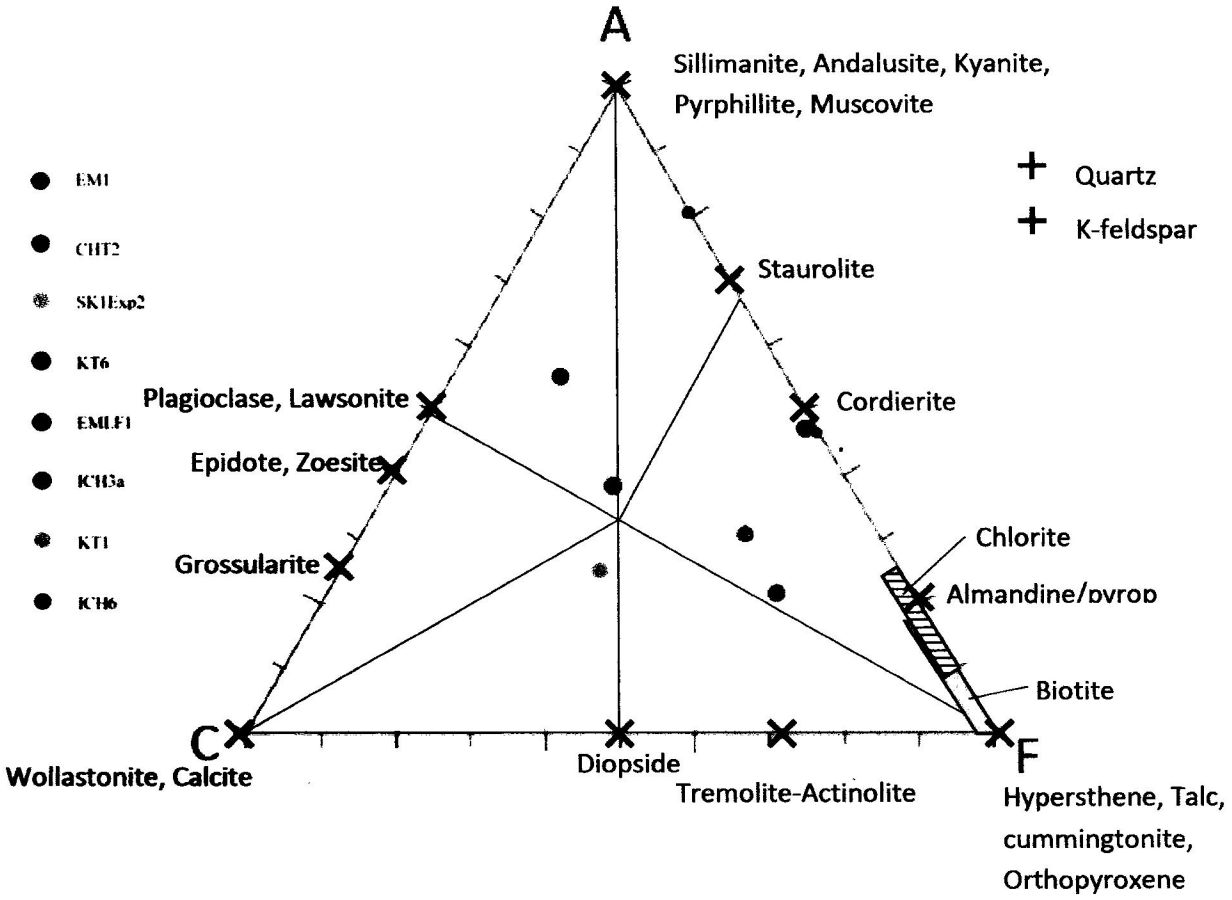

Figure 4.21: ACF diagram representing Mineral Assemblages (Winkler, 1967)

CHAPTER FIVE

5.0 Conclusions and Recommendations

5.1 Conclusions

The result of geochemical (major oxides) analyses of the rocks in the Shintaku area shows that the protolith of these rocks are Al-rich clays, clays and shales either free of carbonate or containing up to 35-65% carbonates and graywackes (using the ACF diagram) which were deposited in an intracratonic basin. The K_2O+Na_2O vs SiO_2 plot shows that the rocks samples analysed were product of tholeiitic magma.

The sequence of entry of the index minerals Garnet-Staurolite-Cordierite (Fig. 4.19) into the pelitic assemblages of the Shintaku area indicates that metamorphic facies ranges from Greenschist facies to the Amphibolite facies.

The major trend of the foliation lies within NNE/SSW direction which indicates that the rocks of the area were formed as a result of the Pan African Orogeny (Ekwueme, 1983).

The major rock types in the studied area are Migmatite, Gneiss, Granite and Schist.

5.2 Recommendations

More work should be done in study area by analyzing more samples for detailed information on the rocks of the Shintaku area.

Geochronological studies should be done on the rocks in the study area to ascertain the age of each rock types to determine their time of formation. Stable isotope studies should also be carried out to determine the barometric and thermometric that is, the pressure and temperature at which these rocks were formed thereby determining the metamorphic facies.

J.A., 1996. The Nigerian Schist belts: Age and depositional environment implication **associated** banded iron-formations. Journal of Mining and Geology. vol. 32, pp. 27-

D. R. (1976). The Geology of the Middle Niger Basin. In: C.A. Kogbe (ed) The Geology **of Nigeria, Univ.** Ife., pp. 283-287.

A.C. and Wright J.B., (1989). The Togo – Benin Nigerian Shied. Evidence of Crustal **aggregation in the** Pan – Africa belt Tectonophysics vol. 165, pp. 125-129.

A.C. Woakes, M. and Rahaman, M.A. (1987): Proterozoic Crustal Development in the **– African** Region of Nigeria, Copyright of the American geophysical Union.

D.M., (1978). Metamorphic bathozones and bathograds: a measure of the depth of **metamorphic** uplift and erosion on the regional scale. Am.J. Sci. pp. 278, 769-797.

C. R and Jones, (1965). An Interpretation of the Geology and Gravity Anomalies of the **Valley,** Nigeria. [Overseas Geological Surveys. Gefophysical Paper. No. 1.]

U.A. (1999). Geotectonic Evolution of the Kazaure Schist belt and Adjacent Areas. **Unpublished.** PhD. Thesis A.B.U. Zaria.

B.N., (2002). Petrogenesis of Schist in Southeast Lokoja, Central Nigeria. Global **of geological** sciences, vol. 1, no. 1, pp 29-42.ff

B.N., (1983). Regional metamorphism of peitic rocks, southeast of Lokoja, Nigeria

B.N., (1981). Mineralogy and petrology of the metamorphosed rocks in south-east **Nigeria.** M.Phil. dissert. Univ. of Nigeria. pp. 99.

of Aviation, (2007). en.m.wikipedia.org. 20/02/2019: 12:50pm

M.R., Agbede, A.C., Egbuniwe I.G., Holt, R and Wright, J.B., (1985). Late Proterozoic **schist belt and plutonism** in NW Nigeria, vol. 142, pp. 319-337

R.M., and Mackenzie F.T., (1971). Evolution of sedimentary rocks. Norton and Co., **New York, pp 394**

T.N., and Baragar, W.R.A., (1971). A guide to the chemical classification of the common **volcanic rocks:** Canadian Journal of Earth Sciences, vol. 8, pp. 523-548.

Leake, B.E. and Singh, D. (1986). The Delaney Dome Formation, Connemara, W. Ireland and the geochemical distinction of ortho and para - quartzofeldspathic rocks. Min. Magz. vol. 50, pp. 205-215.

McCurry, P. (1989). Geology of the Precambrian to Lower Paleozoic Rocks of NW Nigeria, a review: In C.A. Kogbe (Ed) Geology of Nigeria, Elizabethan publ. Lagos, Nig. pp. 15-39.

McCurry, P., (1976). The Geology of the Precambrian to Lower Paleozoic rocks of Northern Nigerian, a Review in C. A., Kogbe (Ed.), Geology of Nigeria pp. 15-39.

McCurry, P. (1971). Pan African Orogemy in Northern Nigeria. Geology. Soc. Amer. Bull. vol. 82, pp. 351 – 61.

ng.geoview.info. 19/02/2019: 02:50pm

Ojo, S.B. and Ajakaiye, D.E., (1976). Preliminary interpretation of gravity measurements in the Middle Niger Basin area, Nigeria. In C.A. Kogbe (editor) Geology of Nigeria pp. 295 – 307.

Rahaman M. A. (1976): Review of the Basement Geology of SW Nigeria in Geology of Nigeria. Elizabethan Publishing Company, Nigeria. pp. 41-58.

Rahaman, M.A and Ocan, O.O. (1978). On relationship in the Precambrian migmatitic gneisses of Nigeria J. Min. and Geol. vol. 15, no.1 (abs).

Telford, W., Geldart, L., Sheriff, R., and Keys, D., (1976). Applied Geophysics, Cambridge University Press, New York.

Tuner, D. C., (1983) Upper Paleozoic Schist belts in the Nigeria Sector of the Pan – Africa provinces of West Africa, Precambrian Research. vol. 21, pp. 55-75.

Winkler, H.G.F., (1967). Petrogenesis of metamorphic rocks. Spinger Verlag, Newyork, 3rd ed., pp. 237. Adekoye J.A. (1996). The Nigerian Schist belt. Age and Deposition of Environment Implication from Associated Banded iron – Formation. Journal. Min. Geology. vol. 32, no. 1, pp. 55 – 46.

Winkler, H.G.F., (1965). Petrogenesis of metamorphic rocks (1st.edn). Springer, New York.

Appendix 1: Result of rock samples analysis

ELEMENT	OXIDE CONVERSION	CHT2	NORMALIZED
Mg	MgO	0.0397968	0.033079529
Na	Na_2O	0.031128	0.025873943
Al	Al_2O_3	13.999433	11.63647981
Si	SiO_2	69.089723	57.42812261
P	P_2O_5	1.273773	1.05877383
S	SO_3	0.8871632	0.73741964
K	K_2O	4.0109136	3.333914604
Ca	CaO	4.4250735	3.678168777
Na	Na_2O	0.0311	0.025850655
Ti	TiO_2	0.5619589	0.467106325
V	V_2O_5	0.0842601	0.070037933
Cr	Cr_2O_3	0.0461853	0.038389741
Mn	MnO	0.0838003	0.069655734
Co	CoO	0.1785169	0.148385202
Fe	Fe_2O_3	11.885392	9.879266326
Fe	FeO	10.694675	8.889528775
Ni	NiO	0.0648987	0.053944505
Cu	CuO	0.0478187	0.039747452
Zn	ZnO	0.0965931	0.080289228
As	As_2O_3	0	0
Pb	PbO_2	0.0258595	0.021494679
W	WO_3	0.0329138	0.027358321
Au	Au_2O	0.0020812	0.001729905
Ag	Ag_2O	0	0
Rb	Rb_2O	0.0840979	0.069903117
Nb	Nb_2O_5	0.075103	0.062426422
Mo	MoO_3	0.3114592	0.258888227
Cd	CdO	0	0
Sn	SnO_2	1.2087856	1.004755649
Sb	Sb_2O_3	1.0339243	0.859409053

ELEMENT	OXIDE CONVERSION	EM1	NORMALIZED
Mg	MgO	0.06765456	0.053590375
Na	Na_2O	0.013889792	0.01100235
Al	Al_2O_3	13.03580538	10.32589237
Si	SiO_2	91.30070169	72.32090316
P	P_2O_5	0.326749462	0.258824037
S	SO_3	0.922869485	0.731021267
K	K_2O	5.197070444	4.116691563
Ca	CaO	0.462012033	0.365967916
Ti	TiO_2	0	0
V	V_2O_5	0.00839031	0.006646113
Cr	Cr_2O_3	0.004092371	0.00324164
Mn	MnO	0.052423624	0.041525681
Co	CoO	0.02898993	0.022963437
Fe	Fe_2O_3	6.076662425	4.813431952
Fe	FeO	5.4678823	4.331206431
Ni	NiO	0.061081136	0.04838345
Cu	CuO	0.038355423	0.030540434
Zn	ZnO	0.093605686	0.074146722
As	As_2O_3	0	0
Pb	PbO_2	0.0117753	0.009327424
W	WO_3	0.034048778	0.02697064
Au	Au_2O	0.141312605	0.111936218
Ag	Ag_2O	0	0
Rb	Rb_2O	0.199472884	0.158006005
Nb	Nb_2O_5	0.024891279	0.019716823
Mo	MoO_3	0.284604075	0.225439929
Cd	CdO	0	0
Sn	SnO_2	1.287500793	1.019852186
Sb	Sb_2O_3	1.101820974	0.872771912

ELEMENT	OXIDE CONVERSION	EMLF1	NORMALIZED
Mg	MgO	0.0596952	0.049770183
Na	Na_2O	0.007006904	0.005841925
Al	Al_2O_3	16.66735947	13.89621817
Si	SiO_2	42.16990416	35.15866981
P	P_2O_5	0.318729664	0.265737171
S	SO_3	0.955329721	0.796495105
K	K_2O	4.152091163	3.46175798
Ca	CaO	5.465929761	4.557155714
Ti	TiO_2	0.748944972	0.624424207
V	V_2O_5	0.044450792	0.037060334
Cr	Cr_2O_3	0.028792751	0.024005623
Mn	MnO	0.122536994	0.102163801
Co	CoO	0.456337097	0.380465776
Fe	Fe_2O_3	24.22000772	20.19315128
Fe	FeO	21.7935673	18.17013465
Ni	NiO	0.085768095	0.071508157
Cu	CuO	0.099768417	0.083180764
Zn	ZnO	0.133686844	0.11145986
As	As_2O_3	0	0
Pb	PbO_2	0.02020272	0.016843784
W	WO_3	0.138465031	0.115443618
Ag	Ag_2O	0	0
Rb	Rb_2O	0.028542995	0.023797392
Nb	Nb_2O_5	0.01459144	0.012165444
Mo	MoO_3	0.292405557	0.243789751
Cd	CdO	0	0
Sn	SnO_2	1.014409954	0.845752565
Sb	Sb_2O_3	0.90316931	0.753006965

ELEMENT	OXIDE CONVERSION	ICH 3a	NORMALIZED
Mg	MgO	0.02785776	0.022753805
Na	Na_2O	0.004309556	0.003519981
Al	Al_2O_3	15.03448276	12.27994235
Si	SiO_2	89.08758343	72.76541577
P	P_2O_5	1.232986573	1.007085131
S	SO_3	1.284925966	1.049508456
K	K_2O	1.248674954	1.019899168
Ca	CaO	5.688260809	4.646086995
Ti	TiO_2	0	0
V	V_2O_5	0.015888034	0.01297711
Cr	Cr_2O_3	0	0
Mn	MnO	0.080314025	0.065599303
Co	CoO	0.00648459	0.005296517
Fe	Fe_2O_3	2.684328668	2.192519811
Fe	FeO	2.41540375	1.97286593
Ni	NiO	0.06668024	0.05446343
Cu	CuO	0.041935282	0.034252116
Zn	ZnO	0.105679824	0.086317712
As	As_2O_3	0	0
Pb	PbO_2	0.0039251	0.003205963
W	WO_3	0.060405054	0.049337951
Au	Au_2O	0	0
Ag	Ag_2O	0.000966744	0.000789622
Rb	Rb_2O	0.006342888	0.005180777
Nb	Nb_2O_5	0.031185626	0.025471956
Mo	MoO_3	0.328412398	0.268242372
Sn	SnO_2	1.584460103	1.294163493
Sb	Sb_2O_3	1.389721936	1.135104249

ELEMENT	OXIDE CONVERSION	ICH6	NORMALIZED
Mg	MgO	0.0198984	0.019075297
Na	Na_2O	0.0031004	0.002972151
Al	Al_2O_3	13.50458196	12.94596099
Si	SiO_2	76.82141023	73.64367018
P	P_2O_5	0.296503368	0.28423842
S	SO_3	0.806012635	0.772671687
K	K_2O	5.973908644	5.726796169
Ca	CaO	0.26332727	0.252434661
Ti	TiO_2	0	0
V	V_2O_5	0.009104379	0.008727774
Cr	Cr_2O_3	0	0
Mn	MnO	0.021950779	0.021042779
Co	CoO	0.005594548	0.005363128
Fe	Fe_2O_3	1.305634588	1.251626632
Fe	FeO	1.1748318	1.12623454
Ni	NiO	0.072279344	0.069289488
Cu	CuO	0.056956876	0.054600838
Zn	ZnO	0.111903606	0.107274681
As	As_2O_3	0	0
Pb	PbO_2	0.048140195	0.046148862
W	WO_3	0	0
Au	Au_2O	0.12747271	0.122199764
Ag	Ag_2O	0	0
Rb	Rb_2O	0.285320589	0.27351822
Nb	Nb_2O_5	0.089122225	0.085435658
Mo	MoO_3	0.20883968	0.200200966
Cd	CdO	0	0
Sn	SnO_2	1.63651368	1.568818814
Sb	Sb_2O_3	1.472613421	1.411698337

ELEMENT	OXIDE CONVERSION	KT6	NORMALIZED
Mg	MgO	0.06367488	0.054919806
Na	Na_2O	0.047033068	0.040566185
Al	Al_2O_3	13.52668871	11.66681619
Si	SiO_2	76.58908095	66.05834947
P	P_2O_5	0.404426928	0.348819636
S	SO_3	0.770306375	0.664391935
K	K_2O	2.335694324	2.014544502
Ca	CaO	5.812088988	5.012947025
Ti	TiO_2	0.018348318	0.015825488
V	V_2O_5	0.020350965	0.017552778
Cr	Cr_2O_3	0.010523239	0.00907633
Mn	MnO	0.049324691	0.042542718
Co	CoO	0.051113824	0.044085851
Fe	Fe_2O_3	6.704173398	5.78237294
Fe	FeO	6.03252715	5.203075709
Ni	NiO	0.075587906	0.065194833
Cu	CuO	0.059460474	0.051284866
Zn	ZnO	0.119123194	0.10274417
As	As_2O_3	0	0
Pb	PbO_2	0.010620858	0.009160527
W	WO_3	0.08827461	0.076137159
Au	Au_2O	0.123622514	0.10662485
Ag	Ag_2O	0.00483372	0.0041691
Rb	Rb_2O	0.015857219	0.013676907
Nb	Nb_2O_5	0.01802472	0.015546384
Mo	MoO_3	0.257748972	0.222309387
Cd	CdO	0.00022847	0.000197056
Sn	SnO_2	1.429949851	1.233336734
Sb	Sb_2O_3	1.302871812	1.123731482

ELEMENT	OXIDE CONVERSION	KT1	NORMALIZED
Mg	MgO	0.02387808	0.017376906
Na	Na_2O	0.01198548	0.008722249
Al	Al_2O_3	11.56088805	8.413258596
Si	SiO_2	105.5763307	76.83155204
P	P_2O_5	0.344163879	0.250459973
S	SO_3	0.480161802	0.349430372
K	K_2O	4.569601041	3.325456926
Ca	CaO	0.407023926	0.296205406
Ti	TiO_2	0.014345048	0.010439388
V	V_2O_5	0.014459896	0.010522967
Cr	Cr_2O_3	0.002046185	0.00148908
Mn	MnO	0.045709268	0.033264217
Co	CoO	0.040560472	0.02951726
Fe	Fe_2O_3	5.864489656	4.267792214
Fe	FeO	5.2769657	3.840230685
Ni	NiO	0.060572127	0.044080434
Cu	CuO	0.035676285	0.025962868
Zn	ZnO	0.089871417	0.065402542
As	As_2O_3	0	0
Pb	PbO_2	0.02666759	0.019406929
W	WO_3	0.063557719	0.046253153
Au	Au_2O	0.071696896	0.052176314
Ag	Ag_2O	0	0
Rb	Rb_2O	0.12270207	0.089294546
Nb	Nb_2O_5	0.009727626	0.00707913
Mo	MoO_3	0.267800882	0.194887976
Cd	CdO	0	0
Sn	SnO_2	1.284199835	0.934556693
Sb	Sb_2O_3	1.14764521	0.835181163

ELEMENT	OXIDE CONVERSION	SK1 Ezp 2	NORMALIZED
Mg	MgO	0.06367488	0.052985371
Na	Na_2O	0.009177184	0.007636552
Al	Al_2O_3	8.629570146	7.180869087
Si	SiO_2	30.68650522	25.53496559
P	P_2O_5	0.459648962	0.382484755
S	SO_3	0.844215836	0.702491931
K	K_2O	2.994723909	2.491980479
Ca	CaO	31.25423255	26.00738491
Ti	TiO_2	0.713415956	0.593650263
V	V_2O_5	0.043558206	0.036245812
Cr	Cr_2O_3	0.025869629	0.021526729
Mn	MnO	0.195232807	0.162457829
Co	CoO	0.34762486	0.289266854
Fe	Fe_2O_3	21.74885264	18.09773383
Fe	FeO	19.5699807	16.28464304
Ni	NiO	0.069734297	0.058027555
Cu	CuO	0.037178444	0.030937061
Zn	ZnO	0.105928775	0.088145835
As	As_2O_3	0	0
Pb	PbO_2	0.009697306	0.008069357
W	WO_3	0.129889783	0.108084355
Au	Au_2O	0	0
Ag	Ag_2O	0.0026854	0.002234585
Rb	Rb_2O	0.136700167	0.113751437
Nb	Nb_2O_5	0.011301213	0.009404006
Mo	MoO_3	0.299456897	0.249185155
Cd	CdO	0	0
Sn	SnO_2	0.963879896	0.802067221
Sb	Sb_2O_3	0.821717329	0.683770393

Appendix 2

Niggli calculations for the data gotten from sample ICH6

ICH6				
	Mol. proportion	**Mol. proportion x 1000**	**Groupings Multiply by factor 100/224.6= 0.445**	
Al_2O_3	12.95	127.19	127.19(0.445)	al=57
Fe_2O_3	1.25	7.83 X 2=15.66	15.66	fm=14
FeO	1.13	15.69	15.69	
MgO	0.02	0.49	0.49	
MnO	0.02	0.28	0.28 — 32.12(0.445)	
CaO	0.25	4.46	4.46 (0.445)	C=2
Na_2O	0.00	0	0	alk=27
K_2O	5.73	60.83	60.83 — 60.83 (0.445)	
			224.6	100%

Niggli calculations for the data gotten from sample KT1

KT1				
	Mol. proportion	**Mol. proportion x 1000**	**Groupings Multiply by factor 100/413.07= 0.242**	
Al_2O_3	8.41	82.59	82.59 (0.242)	al=20
Fe_2O_3	4.27	26.74 X 2	53.48	fm=70
FeO	3.84	48.33	48.33	
MgO	0.02	0.49	0.49	
MnO	0.03	187.5	187.5 — 289.8 (0.242)	
CaO	0.29	5.17	5.17 (0.242)	C=1
Na_2O	0.01	0.16	0.16	alk=9
K_2O	3.33	35.35	35.35 — 35.51 (0.242)	
			413.07	100%

Niggli calculations for the data gotten from sample EM1

EM1				
	Mol. proportion	**Mol. proportion x 1000**	**Groupings Multiply by factor 100/272.6= 0.367**	
Al_2O_3	10.32	101	101 (0.367)	al=37.1
Fe_2O_3	4.81	30 X 2	121.5 (0.367)	fm=44.6
FeO	4.33	60		
MgO	0.05	1		
MnO	0.04	0.5		
CaO	0.36	6	6 (0.367)	C=2.2
Na_2O	0.01	0.1	44.1 (0.367)	alk=16.2
K_2O	4.11	44		
			272.6	100.1%

Niggli calculations for the data gotten from sample CHT2

CHT2	Mol. proportion	Mol. proportion x 1000	Groupings Multiply by factor 100/455.71= 0.219	
Al_2O_3	11.64	114.3	114.3 (0.219)	al= 25.08
Fe_2O_3	9.88	61.87 X 2	247.94 (0.219)	fm=54.29
FeO	8.89	123.47		
MgO	0.03	0.74		
MnO	0.07	0.99		
CaO	3.68	56.63	56.63 (0.219)	C=12.40
Na_2O	0.03	0.49	35.84 (0.219)	alk=7.84
K_2O	3.33	35.35		
			455.71	100.3%

Niggli calculations for the data gotten from sample EMLF1

EMLF1	Mol. proportion	Mol. proportion x 1000	Groupings Multiply by factor 100/762.61= 0.131	
Al_2O_3	13.89	136.42	136.42 (0.131)	al= 17.9
Fe_2O_3	20.19	126.44 X 2	507.97 (0.131)	fm= 66.9
FeO	18.17	252.36		
MgO	0.05	1.24		
MnO	0.10	1.41		
CaO	4.56	81.33	81.33 (0.131)	C= 10.6
Na_2O	0.01	0.16	36.89 (0.131)	alk=4.8
K_2O	3.46	36.73		
			762.61	100.3%

Niggli calculations for the data gotten from sample ICH3a

ICH3a	Mol. proportion	Mol. proportion x 1000	Groupings Multiply by factor 100/270.62= 0.369	
Al_2O_3	12.28	120.60	120.60 (0.369)	al= 44.5
Fe_2O_3	2.19	13.71 X 2	56.26 (0.369)	fm= 20.8
FeO	1.97	27.36		
MgO	0.02	O.49		
MnO	0.07	0.99		
CaO	4.65	82.93	82.93 (0.369)	C= 30.6
Na_2O	0.00	0	10.83 (0.369)	alk=4.00
K_2O	1.01	10.83		
			270.62	99.9%

Niggli calculations for the data gotten from sample SK1Exp2

SK1Exp2	Mol. proportion	Mol. proportion x 1000	Groupings Multiply by factor 100/1017.2= 0.098	
Al_2O_3	7.18	70.5	70.5 (0.098)	al= 6.9
Fe_2O_3	18.09	113.3 X 2	456.2 (0.098)	fm= 44.7
FeO	16.28	226.1		
MgO	0.05	1.2		
MnO	0.16	2.3		
CaO	26.01	463.9	463.9 (0.098)	C= 45.5
Na_2O	0.01	0.2	26.6 (0.098)	alk= 2.6
K_2O	2.49	26.4		
			1017.2	99.7%

Niggli calculations for the data gotten from sample KT6

KT6	Mol. proportion	Mol. proportion x 1000	Groupings Multiply by factor 100/372.35 = 0.268	
Al_2O_3	11.67	114.61	114.61 (0.268)	al= 30.7
Fe_2O_3	5.78	36.19 X 2	146.4 (0.268)	fm= 39.3
FeO	5.20	72.22		
MgO	0.05	1.24		
MnO	0.04	0.56		
CaO	5.01	89.35	89.35 (0.268)	C= 23.9
Na_2O	0.04	0.65	21.99 (0.268)	alk= 5.9
K_2O	2.10	21.34		
			372.35	99.8%

Appendix 3

Calculations showing the data used in plotting **al-alk vs C**

SAMPLE	al-alk	C
EM1	37.1-16.2=20.9	2.2
CHT2	25.08-7.84=17.2	12.40
SK1Exp	6.9-2.6=4.3	45.5
KT6	30.7-5.9=24.8	23.9
EMLF	17.9-4.8=13.1	10.6
ICH3a	44.5-4.00=40.5	30.6
KT1	20-9= 11	1
ICH6	57-27=30	2

Appendix 4

Calculations showing the data used in plotting **Na_2O+K_2O vs Silica**

SAMPLES	**Na_2O+K_2O**	**Silica**
EM1	0.01+4.11=4.12	72.3
CHT2	0.03+3.33=3.36	57.4
SK1Exp2	0.01+2.49=2.5	25.5
KT6	0.04+2.01=2.1	66.1
EMLF1	0.01+3.46=3.5	35.2
ICH3a	0.0035+1.02=1.02	72.8
KT1	0.01+3.33=3.34	76.8
ICH6	0.003+5.73=5.73	73.6

Appendix 5

Calculations showing the data used in plotting Na_2O/Al_2O_3 versus K_2O/Al_2O_3 diagram

SAMPLES	Na_2O/Al_2O_3	K_2O/Al_2O_3
EM1	0.01/10.32=0	4.11/10.32=0.3983
CHT2	0.03/11.64=0.0026	3.33/11.64=0.2861
SK1Exp2	0.01/7.18=0.0014	2.49/7.18=0.3468
KT6	0.04/11.67=0.0034	2.01/11.67=0.1722
EMLF1	0.01/13.89=0.0007	3.46/13.89=0.2491
ICH3a	0.0035/12.28=0.0003	1.02/12.28=0.0831
KT1	0.01/8.41=0.00012	3.33/8.41=0.3959
ICH6	0.0003/12.95=0.0002	5.73/12.95=0.4425